Universiteit Leiden
The Netherlands

Ruthenium-peptide conjugates for targeted phototherapy

Zhang, I.

Citation
Zhang, I. (2023, July 4). *Ruthenium-peptide conjugates for targeted phototherapy*. Retrieved from https://hdl.handle.net/1887/3628436

Version:	Publisher's Version
License:	Licence agreement concerning inclusion of doctoral thesis in the Institutional Repository of the University of Leiden
Downloaded from:	https://hdl.handle.net/1887/3628436

Note: To cite this publication please use the final published version (if applicable).

6

Conclusion

&

Discussion

&

Outlook

6.1 Conclusion

In this PhD thesis, a series of Ru(II) polypyridine-peptide conjugates were presented that differed in their polypyridine ligand, peptide sequence, and/or chirality at the metal center or on the amino acids. Their structure, photochemistry, *in vitro* cellular behaviors, and *in vivo* antitumor efficiency and biodistribution, were studied and compared. The direct coordination of histidine or methionine residues to a racemic ruthenium(II) precursor allows for easy synthesis of the conjugate compounds, but requires HPLC separation of the different diastereomers of the product. Our strategy of coordinating a bidentate peptide directly to a metal center to afford a metal-containing cyclic peptide offers an alternative for the traditional conjugation strategy *via* covalent-bond formation on a spectator ligand. In principle, when the proper amino-acid residues (*i.e.,* histidine or methionine) is included in the peptide sequence, the metal-peptide conjugate can be prepared using comparatively mild reaction conditions.

The attachment of a peptide to a metallodrug has several purposes as discussed in this thesis. First, it shields the cytotoxic metal species (e.g., $[Ru(Ph_2phen)_2(H_2O)_2]^{2+}$ in **Chapter 3** and **5**) by preventing its binding to biomolecules, and it increases its biocompatibility, thus leading to low systemic toxicity in the dark. Upon light irradiation, however, the peptide from **$[Ru(Ph_2phen)_2$(Ac-MRGDH-$NH_2)]Cl_2$** or **$[Ru(Ph_2phen)_2$(Ac-MRGDM-$NH_2)]Cl_2$** was effectively dissociated by two well-defined photochemical steps, releasing the toxic ruthenium compound that kills cancer cells with high efficiency. Second, the peptide acts as a tumor-targeting motif, resulting in strong binding of the conjugate to integrin (e.g., $K_a = 7.0\times10^7\ M^{-1}$ for the binding of Λ-**$[Ru(Ph_2phen)_2$(Ac-MRGDH-$NH_2)]Cl_2$** to $\alpha_{IIb}\beta_3$, **Chapter 3**). Through receptor-mediated uptake, the ruthenium peptide conjugate showed higher uptake efficiency *in vitro* than complex that was not conjugated to a peptide (**Chapter 2**). In addition, high intracellular ruthenium accumulation was detected in cell lines that overexpressed integrin $\alpha_v\beta_3$ and $\alpha_v\beta_5$, e.g., human primary glioblastoma U87MG cells. Third, but most importantly, the Ru-peptide conjugates showed low toxicity in animals and promising light-activated potency against brain tumor, according to the results of the *in vivo* studies using subcutaneous glioblastoma nude mice model (**Chapter 3**) and zebrafish glioblastoma xenograft model (**Chapter 4**). Prodrug accumulation occurred in the tumor, revealing an outstanding capability to cross the blood brain barrier (BBB).

Besides photochemical and biological properties, the influence of the coordinating residues in the peptide towards the configuration of the ruthenium conjugate, was also addressed. When using a racemic precursor, *i.e., cis*-$[Ru(Ph_2phen)_2Cl_2]$, and different peptides, *i.e.,* Ac-HRGDH-

NH_2, Ac-MRGDH-NH_2 and Ac-MRGDM-NH_2, the ratio between the Λ and Δ isomers of the resulting Ru-peptide conjugates **[Ru(Ph$_2$phen)$_2$(Ac-HRGDH-NH$_2$)]Cl$_2$**, **[Ru(Ph$_2$phen)$_2$(Ac-MRGDH-NH$_2$)]Cl$_2$** and **[Ru(Ph$_2$phen)$_2$(Ac-MRGDM-NH$_2$)]Cl$_2$** was 1:2, 1:1.5 and 1:1, respectively (**Chapter 4**). It seems that the higher rigidity of histidine residues, compared to methionines,[1] promotes the formation of a higher fraction of the Δ-isomer, while for the more flexible **[Ru(Ph$_2$phen)$_2$(Ac-MRGDM-NH$_2$)]Cl$_2$** conjugate there is little to no energetic preference for one or the other diastereoisomer, thus resulting in a 1:1 ratio of the isomers. Furthermore, when one of the enantiomerically pure L (Ac-MRGDM-NH_2, called **p1**), D (Ac-mrGdm-NH_2, **p2**), or L/D (Ac-MrGdM-NH_2, **p3**) peptide was coordinated with racemic *cis*-[Ru(Ph$_2$phen)$_2$Cl$_2$], the ratio between Λ and Δ isomers of the resulting Ru-peptide conjugates [Ru(Ph$_2$phen)$_2$(**p1**)]Cl$_2$, [Ru(Ph$_2$phen)$_2$(**p2**)]Cl$_2$ and [Ru(Ph$_2$phen)$_2$(**p3**)]Cl$_2$ also differed, as described in **Chapter 5**. The 1:1 ratio of Δ/Λ isomers from [Ru(Ph$_2$phen)$_2$(**p1**)]Cl$_2$ and [Ru(Ph$_2$phen)$_2$(**p2**)]Cl$_2$ was consistent with the use of a racemic *cis*-[Ru(Ph$_2$phen)$_2$Cl$_2$] precursor and mirror image peptides **p1** and **p2**. For [Ru(Ph$_2$phen)$_2$(**p3**)]Cl$_2$, a 1:2 ratio of the Δ and Λ diastereomer was obtained, confirming the significant influence of peptide structure on the configuration of the metal center.

In the series of tris(bidentate) octahedral complexes [Ru(N-N)$_2$(peptide)]$^{2+}$ discussed in this thesis, the photochemistry and cellular behavior of the conjugates were shown to be strongly influenced by the structure of the bis-imine spectator ligands N-N. The compounds bearing two bpy or two Ph$_2$phen chelating ligands and the peptide sequence Ac-HRGDH-NH_2 (**Chapter 2**) behave as PDT compounds generating singlet oxygen ($^1O_2$) and phosphorescence upon visible light irradiation. With sterically more hindered dmbpy ligands, a PACT ruthenium complex was obtained. Next to the influence of the steric hindrance of the diamine ligands, the nature of the metal-binding amino acid residues on the peptide also appeared to be important. As described in **Chapter 4**, three conjugates **[Ru(Ph$_2$phen)$_2$(Ac-HRGDH-NH$_2$)]Cl$_2$**, **[Ru(Ph$_2$phen)$_2$(Ac-MRGDH-NH$_2$)]Cl$_2$** and **[Ru(Ph$_2$phen)$_2$(Ac-MRGDM-NH$_2$)]Cl$_2$** with different amino-acid residues coordinated to the metal center followed different photoactivated pathways. Following the series **[Ru(Ph$_2$phen)$_2$(Ac-HRGDH-NH$_2$)]Cl$_2$**, **[Ru(Ph$_2$phen)$_2$(Ac-MRGDH-NH$_2$)]Cl$_2$** and **[Ru(Ph$_2$phen)$_2$(Ac-MRGDM-NH$_2$)]Cl$_2$**, the energy gap between the ^{3}MLCT and ^{3}MC states (ΔE=E(^{3}MC)-E(^{3}MLCT)) decreased, as well as the singlet oxygen ($^1O_2$) and superoxide radicals ($O_2^{\bullet-}$) generation, while photosubstitution quantum yields increased. Meanwhile, the cytotoxicity studies under different oxygen conditions showed that, **[Ru(Ph$_2$phen)$_2$(Ac-HRGDH-NH$_2$)]Cl$_2$** lost all phototoxicity in hypoxic (1% O_2) conditions

(PI=1.3 *vs*. 12.1 under normoxia), while **[Ru(Ph$_2$phen)$_2$(Ac-MRGDH-NH$_2$)]Cl$_2$** lost most of its phototoxicity (PI=1.9 *vs*. 11.9 under normoxia), and **[Ru(Ph$_2$phen)$_2$(Ac-MRGDM-NH$_2$)]Cl$_2$** kept a significant phototoxicity (PI=4.0 *vs*. 8.5 under normoxia). These results show that the replacement of histidine coordination sites by methionines turns the Ru-peptide conjugate from a PDT compound (**[Ru(Ph$_2$phen)$_2$(Ac-HRGDH-NH$_2$)]Cl$_2$**) into a PACT compound (**[Ru(Ph$_2$phen)$_2$(Ac-MRGDM-NH$_2$)]Cl$_2$**). Thus, use of methionine donors is advised if one wants to develop PACT ruthenium-peptide conjugates by direct coordination of amino acids.

Intracellular accumulation of Ru-peptide conjugates is a result of multiple factors. First, the relative cellular expression of the targeted receptors, *i.e.,* integrin $\alpha_v\beta_3$ and integrin $\alpha_v\beta_5$, significantly influenced uptake efficiency of the Ru-peptide conjugates, strongly suggesting that the series of Ru-RGD conjugates were internalized by receptor-mediated uptake. As shown in **Chapter 2** (Figure 2.2), ruthenium accumulation e.g. for Δ/Λ mixtures of **[Ru(Ph$_2$phen)$_2$(Ac-HRGDH-NH$_2$)]Cl$_2$** decreased down the series A549-Hypo>A549-Norm>MCF-7-Hypo>MCF-7-Norm, which strikingly corresponds with the trend in cellular integrin $\alpha_v\beta_3$ expression in these cell lines. Similarly, an uptake study using purified Δ- or Λ-**[Ru(Ph$_2$phen)$_2$(Ac-MRGDH-NH$_2$)]Cl$_2$** in U87MG, PC-3 and MCF-7 (**Chapter 3**, Figure 3.5) also confirmed that cell lines with higher integrin $\alpha_v\beta_3$ and integrin $\alpha_v\beta_5$ expression resulted in higher uptake efficiency.

Second, the lipophilicity of the ruthenium compounds is also critical for cellular uptake. The intracellular uptake of **[Ru(Ph$_2$phen)$_2$(Ac-HRGDH-NH$_2$)]Cl$_2$** was much higher than that of **[Ru(bpy)$_2$(Ac-HRGDH-NH$_2$)]Cl$_2$ (Chapter 2)**. Thus, the lipophilic ligand Ph$_2$phen helped the ruthenium complex to enter into cells more efficiently than bpy. Not only the uptake efficiency, but also the intracellular localization differed between these two complexes. The colocalization study showed that **[Ru(Ph$_2$phen)$_2$(Ac-HRGDH-NH$_2$)]Cl$_2$** mainly located in the lysosomes, while **[Ru(bpy)$_2$(Ac-HRGDH-NH$_2$)]Cl$_2$** appeared to reside mainly in the Golgi area. The lipophilicity of the peptide also influences the uptake of the ruthenium compounds as is described in **Chapter 3** for the relatively lipophilic peptide sequence Ac-MRVDH-NH$_2$ compared to Ac-MRGDH-NH$_2$. The corresponding Ru-peptide conjugate **[Ru(Ph$_2$phen)$_2$(Ac-MRVDH-NH$_2$)]Cl$_2$** showed relatively high uptake efficiency and *in vitro* cytotoxicity, even with a reduced binding affinity to integrin $\alpha_{IIb}\beta_3$.

6.2 Discussion

The chirality of the metal center does not have a large influence on the activity of photoactivated chemotherapy (PACT) prodrugs described in this thesis. In **Chapter 3**, we compared the two diastereoisomers: Λ and Δ of the compound **[Ru(Ph$_2$phen)$_2$(Ac-MRGDH-NH$_2$)]Cl$_2$**, no significant differences were found between them, neither in terms of chemistry nor in terms of biology. The association constant (K_a) of Λ-**[Ru(Ph$_2$phen)$_2$(Ac-MRGDH-NH$_2$)]Cl$_2$** with integrin $\alpha_{IIb}\beta_3$ ($7.0 \pm 0.8 \times 10^7\ M^{-1}$) was found to be twice higher than that of the Λ diastereomer ($3.1 \pm 0.2 \times 10^7\ M^{-1}$) (**Chapter 3)**. However, very small differences were observed between both isomers in terms of cytotoxicity (EC_{50} and photo index). Furthermore, pairs of diastereomers were isolated for the compound **[Ru(Ph$_2$phen)$_2$(peptide)]Cl$_2$** with three different peptides Ac-MRGDM-NH_2, Ac-mrGDm-NH_2 and Ac-MrGdM-NH_2. Their photochemistry and cytotoxicity were also studied as described in **Chapter 5**, the difference between the Λ and Δ isomers in each pair were again found not to be significant. As a PACT pathway was involved for these molecules, upon irradiation, the peptide was photosubstituted by two water molecules in two well-identified steps in aqueous solution, and both Λ and Δ configurations ended up with the photoproduct $[Ru(Ph_2phen)_2(H_2O)_2]^{2+}$. The chiral signal of Λ- and Δ-**[Ru(Ph$_2$phen)$_2$(Ac-MRGDH-NH$_2$)]Cl$_2$** in the CD spectra gradually decreased during light activation **(Chapter 3**, Figure 3.2b**)**, demonstrating that photoracemization of the tris-chelated Ru complexes took place in parallel to photosubstitution. Photoracemization has been reported for $[Ru(bpy)_3]^{2+}$ complex and its analogues a long time ago.[2] Thus, for PACT complexes of this kind the chirality of the metal center is not retained during photoactivation, and although ruthenium complexes with different Λ or Δ configuration might have different biological properties as prodrugs, upon light irradiation they will end up as the same racemic mixture of the enantiomers of the photoproduct.

The boundaries between PACT and PDT compounds are hard to identify in biological environments. The three compounds **[Ru(Ph$_2$phen)$_2$(Ac-HRGDH-NH$_2$)]Cl$_2$**, **[Ru(Ph$_2$phen)$_2$(Ac-MRGDH-NH$_2$)]Cl$_2$** and **[Ru(Ph$_2$phen)$_2$(Ac-MRGDM-NH$_2$)]Cl$_2$** were all shown to photosubstitute their RGD peptide, but at very different rates as determined with photochemical studies (**Chapter 4**). The emission and $^1O_2$ generation quantum yields designated **[Ru(Ph$_2$phen)$_2$(Ac-HRGDH-NH$_2$)]Cl$_2$** to be a typical PDT compound, **[Ru(Ph$_2$phen)$_2$(Ac-MRGDH-NH$_2$)]Cl$_2$** as a PACT compound with some photodynamic properties, and **[Ru(Ph$_2$phen)$_2$(Ac-MRGDM-NH$_2$)]Cl$_2$** as a typical PACT compound. **[Ru(Ph$_2$phen)$_2$(Ac-MRGDH-NH$_2$)]Cl$_2$** and **[Ru(Ph$_2$phen)$_2$(Ac-MRGDM-NH$_2$)]Cl$_2$** were

characterized by two relatively high initial photosubstitution quantum yields, low phosphorescence emission, and low singlet oxygen production in the laboratory. However, the behavior of these complexes in biological environments suggested that they do not kill cells *via* a single photoactivated pathway. The photosubstitution products generated in cells were found to be emissive in the red region of the spectrum, and further light irradiation led to significant ROS generation. In other words, they behaved also as PDT compounds. After confirming the photodynamic properties of **[Ru(Ph$_2$phen)$_2$(Ac-HRGDH-NH$_2$)]Cl$_2$**, it is straightforward to hypothesize that the photoproduct [Ru(Ph$_2$phen)$_2$(H$_2$O)]$^{2+}$ of **[Ru(Ph$_2$phen)$_2$(Ac-MRGDH-NH$_2$)]Cl$_2$** or **[Ru(Ph$_2$phen)$_2$(Ac-MRGDM-NH$_2$)]Cl$_2$** can bind to histidine residues in proteins present in cells, leading to secondary histidine-bound, emissive ruthenium species capable of ROS generation. Hence photosubstitution and ROS generation, which are two different types of reactivity typical for PACT and PDT, may combine in a biological environment. They probably contribute both to the phototoxicity observed for these ruthenium-peptide compounds in normoxic conditions. Under hypoxic conditions, however, only PACT may remain operative due to the low concentration of ground-state O_2 in the cells. We hypothesize that this is the reason why **[Ru(Ph$_2$phen)$_2$(Ac-MRGDM-NH$_2$)]Cl$_2$** retains a high PI value under hypoxia, while the PI values for **[Ru(Ph$_2$phen)$_2$(Ac-MRGDH-NH$_2$)]Cl$_2$** and **[Ru(Ph$_2$phen)$_2$(Ac-HRGDH-NH$_2$)]Cl$_2$** are close to unity. However, the PACT compound **Ru-[Ru(Ph$_2$phen)$_2$(Ac-MRGDM-NH$_2$)]Cl$_2$** *turns into* a PDT compound after light activation, which means that the boundaries between PACT and PDT from this complex are permeable. However, this dual action does not always happen. A PACT compound such as [Ru(tpy)(biq)(STF31)]Cl$_2$ relies on the toxicity of the photosubstituted ligand,[3] but the metal-containing photoproduct is so sterically hindered that it cannot bind very well to DNA or proteins, thus negligible ROS production will be observed after light activation. Overall, ROS and phosphorescence detection in cells treated with **[Ru(Ph$_2$phen)$_2$(Ac-MRGDM-NH$_2$)]Cl$_2$**, which initially upon irradiation reacts as a PACT compound, is not a bad thing. Instead it may bring additional phototoxicity towards cancer cells in normoxic conditions.

For PDT or PACT complexes with similar toxicity (i.e. EC$_{50}$ values) *in vitro*, which one works better *in vivo*? The three conjugates **[Ru(Ph$_2$phen)$_2$(Ac-HRGDH-NH$_2$)]Cl$_2$**, **[Ru(Ph$_2$phen)$_2$(Ac-MRGDH-NH$_2$)]Cl$_2$** and **[Ru(Ph$_2$phen)$_2$(Ac-MRGDM-NH$_2$)]Cl$_2$** shared very similar toxicity in normoxic conditions *in vitro,* while **Ru-[Ru(Ph$_2$phen)$_2$(Ac-HRGDH-NH$_2$)]Cl$_2$** and **[Ru(Ph$_2$phen)$_2$(Ac-MRGDH-NH$_2$)]Cl$_2$** in contrast to **[Ru(Ph$_2$phen)$_2$(Ac-MRGDM-NH$_2$)]Cl$_2$** essentially lost their toxicity in hypoxic conditions as their mode of action

depends on the presence of O_2. In a large size of tumors *in vivo*, hypoxic regions are usually developed which can limit the antitumor efficiency of PDT compounds dramatically, at the same time, the hypoxia induced factors (HIF) are also switched on.[4] At that stage, PACT complexes could also be affected by hypoxia-triggered chemoresistance, but normally with reduced toxicity under both dark and light condition, and high photo index is still retained. Besides hypoxia, another factor influencing the efficiency of PDT/PACT *in vivo* is the distribution of the Ru-peptide conjugates in a large tumor. For PDT type II compound, the lifetime of $^1O_2$ is very short (approximately 10-320 ns), leading to a very short diffusion distance in a cell of approximately 10-55 nm.[5] Thus, photodynamic damage will occur very close to where the photosensitizer is physically located.[6] For this reason, deep penetration is very important for the efficacy of photosensitizers, and thus for **[Ru(Ph$_2$phen)$_2$(Ac-HRGDH-NH$_2$)]Cl$_2$** as it works mostly via PDT (**Chapter 4**). On the other hand, **[Ru(Ph$_2$phen)$_2$(Ac-MRGDM-NH$_2$)]Cl$_2$** essentially acts as a PACT compound, upon irradiation the active toxic species $[Ru(Ph_2phen)_2(H_2O)]^{2+}$ is released, its toxicity occurs after interacting with biological targets *i.e.,* DNA or protein. The prodrug of the compound does not necessary have to penetrate as deep into the tumor as a classical PDT compound, provided that the active photoproduct itself can diffuse more deeply into the tumor. Since **[Ru(Ph$_2$phen)$_2$(Ac-HRGDH-NH$_2$)]Cl$_2$** and **[Ru(Ph$_2$phen)$_2$(Ac-MRGDM-NH$_2$)]Cl$_2$** both carry the same targeting motif and have a similar cyclic shape, we assume their penetration into tumors to be quite similar (**Chapter 4**, Figure 4.5). The PACT prodrug **[Ru(Ph$_2$phen)$_2$(Ac-MRGDM-NH$_2$)]Cl$_2$** in theory has higher potential to be phototoxic in larger tumors, as the toxic species is longer lived. In practice, the penetration depth of these compounds in real tissues is still unknown, and specific studies *in vivo* need to be realized to evaluate the relation between prodrug penetration depth and antitumor efficacy.

The three complexes **[Ru(Ph$_2$phen)$_2$(Ac-HRGDH-NH$_2$)]Cl$_2$**, **[Ru(Ph$_2$phen)$_2$(Ac-MRGDH-NH$_2$)]Cl$_2$** and **[Ru(Ph$_2$phen)$_2$(Ac-MRGDM-NH$_2$)]Cl$_2$** were injected into a zebrafish-embryo brain-tumor model, as described in **Chapter 4**. On the one hand, zebrafish embryos are well-described animals that are convenient and versatile xenogeneic models for *in vivo* drug screening of human tumors.[7-9] They are able to mimic the physiological delivery of prodrugs through circulation as in mice or a human patient, allow for localization of emissive drugs in the brain-tumor region by simple fluorescence imaging, and offer a model of the blood-brain barrier. Using this model, we confirmed that in spite of the differences between the three compounds *in vitro*, all of them showed promising and similar antitumor effects in U87MG

brain tumors *in vivo*. However, the tumors in a zebrafish model are very small (~0.0055 mm^3) and hence are not prone to show important hypoxic areas. Questions including: 1) how the efficiency of PDT drug **[Ru(Ph$_2$phen)$_2$(Ac-HRGDH-NH$_2$)]Cl$_2$** is limited in hypoxic tumors, or 2) whether the size of the solid tumors affects the physical penetration of the active species $[Ru(Ph_2phen)_2(H_2O)]^{2+}$ generated by PACT drug **[Ru(Ph$_2$phen)$_2$(Ac-MRGDM-NH$_2$)]Cl$_2$**, could not be answered. Alternatively, a mice model may be a better choice to address the difference between the two pathways affected by real solid tumors, as the tumor size in mice can go up to 500 mm^3 (when drug is injected). We already confirmed that **[Ru(Ph$_2$phen)$_2$(Ac-MRGDH-NH$_2$)]Cl$_2$** efficiently accumulated in U87MG tumors and lowered tumor volume efficiently, by using a heterotopic sub-cutaneous tumor model in mice, as described in **Chapter 3**. Ideally, a comparison of toxicity should be made between **[Ru(Ph$_2$phen)$_2$(Ac-HRGDH-NH$_2$)]Cl$_2$**, **[Ru(Ph$_2$phen)$_2$(Ac-MRGDH-NH$_2$)]Cl$_2$** and **[Ru(Ph$_2$phen)$_2$(Ac-MRGDM-NH$_2$)]Cl$_2$** in mice models, preferably using orthotopic brain tumors. *In vivo* studies using mice models are time consuming and expensive, so it is essential to choose the model that best can answer the question(s) that a PACT researcher wants to probe.

6.3 Outlook

Although light-activatable, metal-based complexes for cancer treatment have developed quickly in the past decades, the number of approved metallodrugs in clinical trials remains quite low. For the development of efficient ruthenium-based PACT complexes, several key requirements need to be met: a suitable light activation window,[10] high photosubstitution efficiency,[1] and very different cytotoxicity in dark and light conditions (high PI value).[11] When considering clinical applications, however, an anticancer drug should also have high solubility in aqueous solutions, good cellular uptake, good stability in biological media, and excellent tumor selectivity.[12] In this thesis, conjugation of an RGD-peptide was confirmed to increase the biocompatibility of ruthenium-based PACT compounds, while providing active tumor targeting to the prodrug. This combination opens new roads towards the future clinical application of Ru-peptide conjugates for PACT treatment of cancer patients. Optimization can be made including the suggestions described in the following sections.

6.3.1 Optimization of the activation wavelength

Even though the use of visible light is already advanced compared to the use of UV light, the optimal wavelength for activation lies in the so-called first phototherapeutic window, which corresponds to ~620-850 nm. Light in this range has the maximum penetration depth in

mammalian tissues and at the same time sufficient energy to trigger photosubstitution.[10, 13] Use of sterically hindered ruthenium photocaging scaffolds $[Ru(tpy)(N\text{-}N)(L)]^{2+}$ (where N-N is a sterically demanding chelating ligand such as dmbpy, biq or dmphen, and L is a thioether ligand) has successfully led to compounds that are activatable with red light, as reported by Turro, Kodanko *et al*,[14-16] as well as our group.[3] The application of two sterically hindered (dmbpy/dmphen/biq) ligands has also proved effective for red light activation of tris(bidentate) ruthenium complexes. The compound $[Ru(biq)_2(phen)]^{2+}$ possesses higher absorption wavelength than for example $[Ru(phen)_2(biq)]^{2+}$, which makes it activatable using red light.[17] The complexes $[Ru(dmbpy)_2(IP\text{-}4T)]^{2+}$ and $[Ru(dmphen)_2(IP\text{-}4T)]^{2+}$ reported by McFarland,[18] showed advanced toxicity upon red light activation. However, the photo-ejected ligand dmbpy or dmphen, is only mildly toxic, and an additional ligand for better biological cytotoxic action should be included in the complex design.

6.3.2 Combination therapy

Monotherapy usually carries as main disadvantage that its efficacy can be overcome by only a few mutations in the tumor DNA, leading to resistance. By contrast, combination of multiple therapeutic modalities holds promises for more efficient anticancer treatment. For example, synergistic combination of photodynamic therapy (PDT) with a chemotherapeutic drug has been reported to improve antitumor efficiency.[19, 20] Typically, the chemotherapy agent may improve the sensitivity of cancer cells to reactive oxygen species (ROS), while, in turn, ROS generated by PDT suppress the chemotherapeutic drug-efflux activity.[21]

One given ruthenium complex in principle can be constructed to show synergetic anticancer properties by combining several biologically active ligands. As shown in Scheme 6.1, a series of ruthenium complexes is proposed that carry four ligands playing different roles. First, a ligand (**R1**) may increase ligand dissociation quantum yields and rates of the complex (here either **R3** or **R4** or both may be substituted). For example, a sterically hindering ligand **R1** such as 2,2'-biquinoline (biq), 6,6'-dimethyl-2,2'-bipyridine (dmbpy) or 2,9-dimethyl-1,10-phenanthroline (dmphen) can be used. Second, the ligand **R2** may bear a ROS-generating group such as benzo[i]dipyrido[3,2-a:2',3'-c]phenazine (dppn) or IP-3T (IP = 1Himidazo[4,5-f][1,10]phenanthroline), which will introduce a photodynamic effect in the complex. The **R3** ligand, e.g., a nicotinamide phosphoribosyltransferase (NAMPT) inhibitor such as STF31,[3] can bring high toxicity to cancer cells after photorelease, which is at the core of PACT. Last but not least, an active targeting motif in **R4**, *i.e.,* an RGD peptide, can bring specific targeting to the

whole molecule, and increase biocompatibility and water solubility of the prodrug, which often becomes problematic when the pi surface of ligands **R1**, **R2**, and **R3** increase.

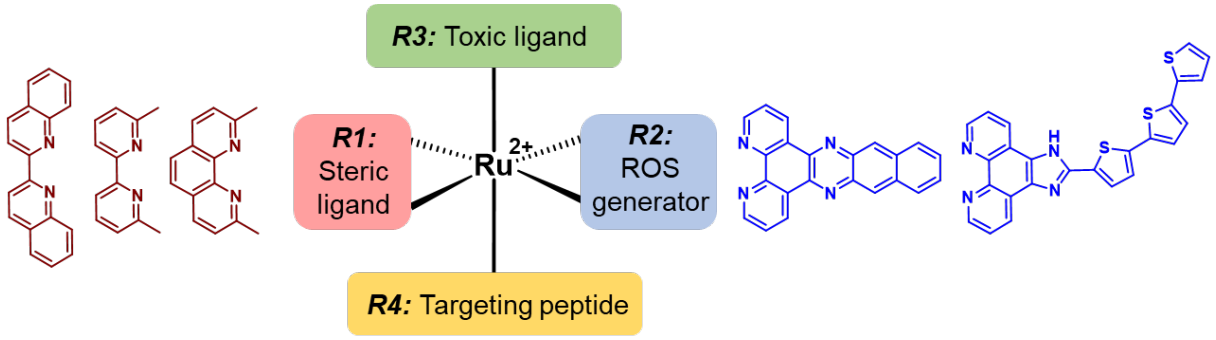

Scheme 6.1. *General design of photoactivated ruthenium complexes for synergetic photodynamic and photoactivated chemotherapy.*

A more direct way to obtain synergistic phototherapy is to treat cancer cells with two types of anticancer drugs, to determine whether the combination will realize more efficient treatment at a given concentration, or the same efficacy but at lower concentrations, compared to each individual treatment. Combination of PDT with PACT, or of either of them with a traditional chemotherapeutic drug, may effectively eliminate tumors at lower doses of the photosensitive prodrugs (in mg/kg) or lower light dose (in J/cm^2), thus minimizing potential side effects to non-malignant tissues.[22] Although synergetic therapy has been studied widely,[23] few reports have been published to date on combination of PDT or PACT and chemotherapeutic drugs. To summarize this approach, we propose to build a database on skin cancer cells for the synergistic combination of drugs (Scheme 6.2). On the one hand, the efficacy of single treatments can be evaluated by measuring EC_{50} values. On the other hand, the drugs with the highest potential are selected to study synergistic effects in Chemo + PDT, Chemo + PACT, and PDT+PACT treatment groups. Following quantitative data analysis,[24] the most promising system(s) will be selected, followed by further mechanistic studies and *in vivo* validation.

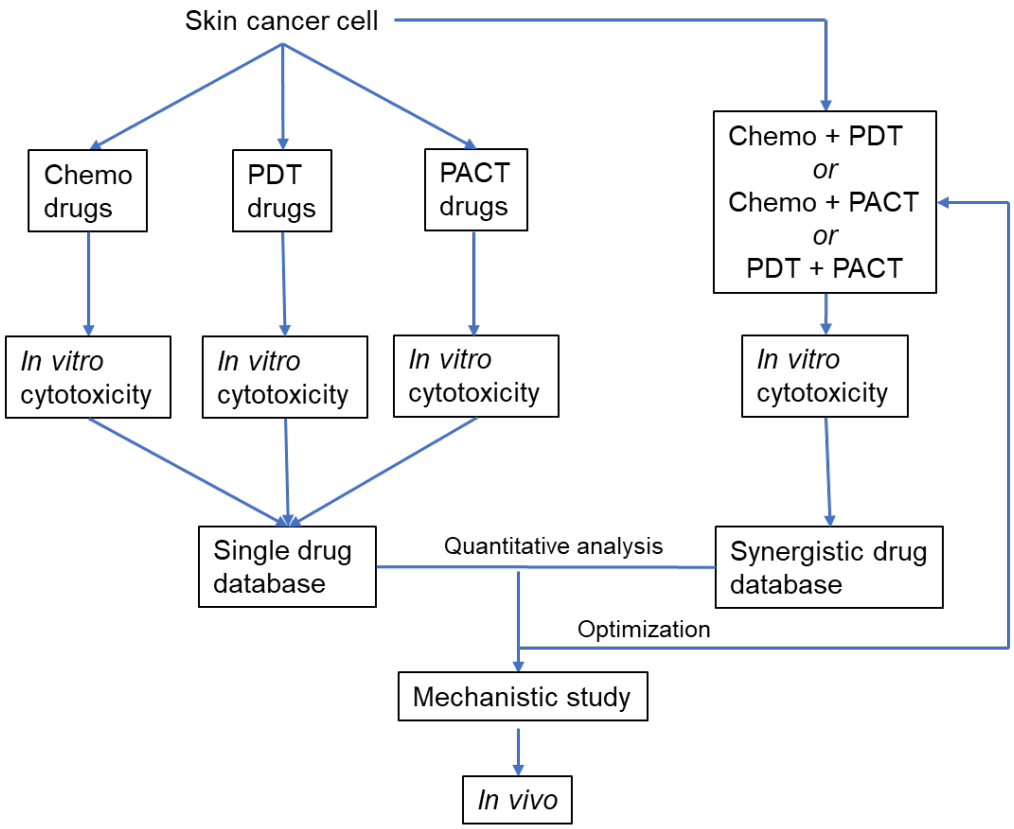

Scheme 6.2. *Simplified flow chart for the analysis of synergistic phototherapy effect.*

6.3.3 Other peptides

In the research described in this thesis, we studied ruthenium conjugates containing targeting peptides based on RGD. However, a large number of peptide-targeting candidates has been developed, especially in relation to cancer, by the development of phage-display combinatorial peptide library or high-throughput sequencing. Examples of such peptide sequences and their corresponding targets are summarized in Table 6.1. This list offers more choices for active tumor targeting by Ru-peptide conjugates for PACT.

Table 6.1. *Examples of peptide sequence for cancer targeting.*

Peptide sequence	Target	Reference
IELLQAR	HL 60 human lymphoma & B-16 mouse melanoma	[25]
VPWMEPAYQRFL	MDA-MB-435 breast cancer	[26]
DPRATPGS	LNCaP prostate cancer	[27]
HLQLQPWYPQIS	WAC-2 human neuroblastoma	[26]
SHWTIDI	protein-95/discslarge/zona occludens-1 (PDZ)	[28]

	glioblastoma	
ATWLPPR/RRKRRR/ASSSY PLIHWRPWAR	Vascular endothelial growth factor (VEGF)	29-31
H-hdwwwinryGkt-NH2	epidermal growth factor (EGF)	32
Cyclic ZD2(CTVRTSADC)	Extradomain-B fibronectin (EDB-FN)	33
HTTIPKV/APPIMSV	Cancer associated fibroblasts (CAFs)	34
ACEEQNPWARYLEWLFPT ERLLLEL	Acidic tumor microenvironment	35

Besides those peptide sequences that target specific receptors, peptides can also be used as delivery vectors for intracellular drug delivery. A group of positively charged peptides such as cell-penetrating peptide (CCP), mitochondria-targeting peptide (MTP) and nuclear location signal (NLS), can be used as carriers to enhance the uptake efficiency of ruthenium complexes. A PACT Ru-NLS conjugate is shown in Scheme 6.3a. By attaching the NLS peptide, the ruthenium complex should become highly soluble in water, and have higher chances to enter the nucleus. After light activation, the peptide will be released and the bis-aqua ruthenium photoproduct can freely bind to DNA and induce cell death.

In addition to cellular targeting or uptake, the peptide ligand can also be used as a "regulator" to change the charge of metal complexes, e.g. using the KDEL peptide, a sequence derived from ER protein.[36] When a Ru(II) complex is bound to the MKDEL peptide (M as coordination site), its overall charge can be altered from 3+ to zero at different pH (Scheme 6.3b). Cancer cells in solid tumors are characterized by an acidic environment,[37] having lower pH in more aggressive tumors. To "target" this specific tumor microenvironment, many pH-sensitive agents have been developed.[38,39] For the complexes shown in Scheme 6.3b, more acidic conditions lead to Ru(II)-MKDEL conjugates carrying more positive charges, which may result in higher cellular uptake.

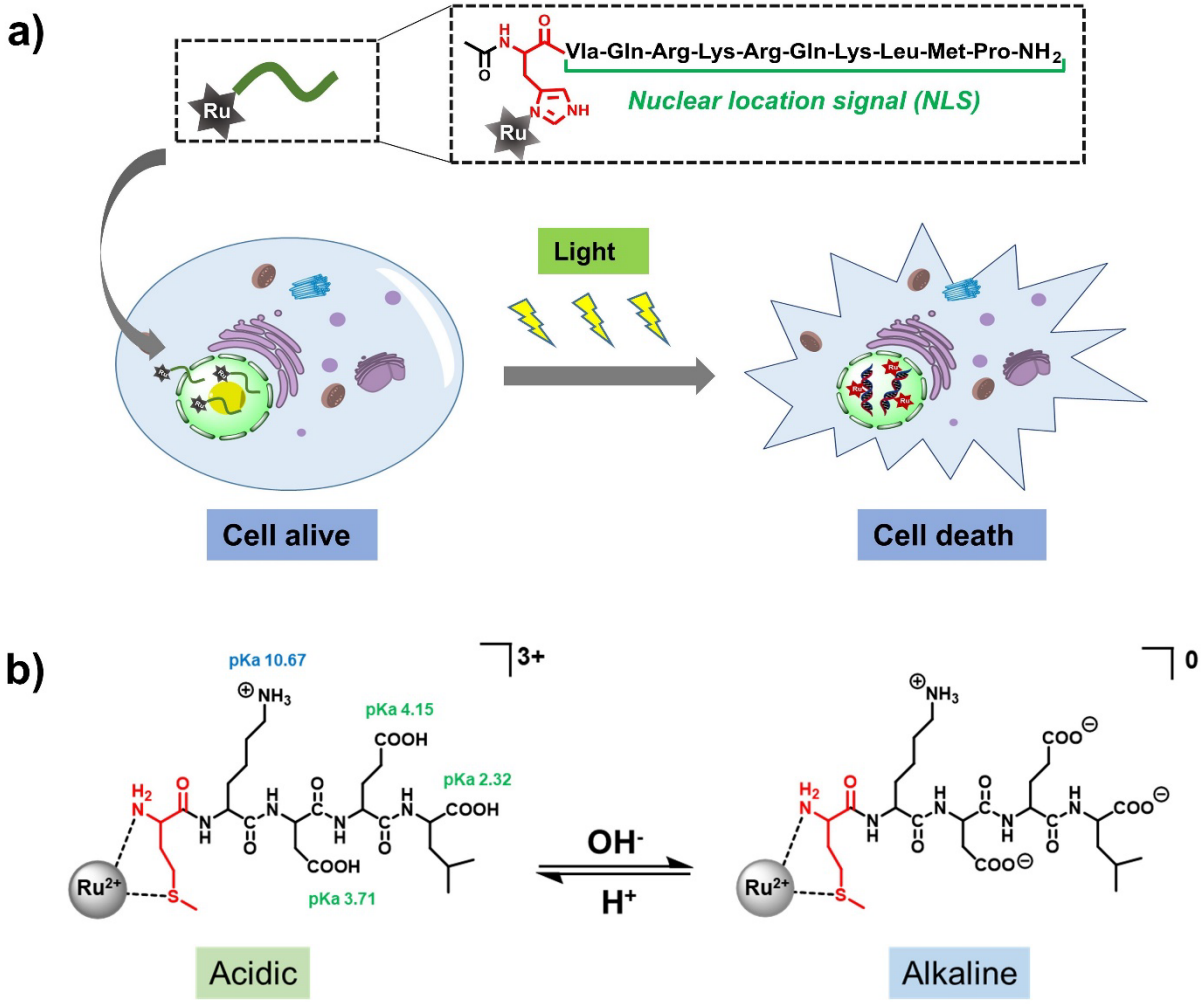

Scheme 6.3. *Examples of Ru-peptide conjugates that were synthesized by author a: $[Ru(bpy)_2(Ac\text{-}HNLS\text{-}NH_2)(H_2O)]^{n+}$ and $[Ru(Ph_2phen)_2(Ac\text{-}HNLS\text{-}NH_2)(H_2O)]^{n+}$, b: $[Ru(Ph_2phen)_2(MKDEL)]^{n+}$, but not described in this thesis.*

In conclusion, the conjugation of peptides with ruthenium complexes represents one of the most promising tools for improving the potential of ruthenium PACT compounds to be used as clinical drugs. Based on the work reported in this thesis, we are convinced that in the near future more Ru-peptide candidates will be developed for active tumor targeting.

6.4 References

1. R. N. Garner, L. E. Joyce and C. Turro, *Inorganic Chemistry*, 2011, **50**, 4384-4391.
2. E. B. Bauer, *Chemical Society Reviews*, 2012, **41**, 3153-3167.
3. L. N. Lameijer, D. Ernst, S. L. Hopkins, M. S. Meijer, S. H. Askes, S. E. Le Dévédec and S. Bonnet, *Angewandte Chemie*, 2017, **129**, 11707-11711.
4. A. Emami Nejad, S. Najafgholian, A. Rostami, A. Sistani, S. Shojaeifar, M. Esparvarinha, R. Nedaeinia, S. Haghjooy Javanmard, M. Taherian and M. Ahmadlou, *Cancer Cell International*, 2021, **21**, 1-26.
5. J. S. Dysart and M. S. Patterson, *Physics in Medicine & Biology*, 2005, **50**, 2597.
6. J. Moan, K. Berg, E. Kvam, A. Western, Z. Malik, A. Rück and H. Schneckenburger, *Photosensitizing Compounds: Their Chemistry, Biology and Clinical Use: Ciba Foundation Symposium 146*. 95-111.
7. L. Chen, A. Groenewoud, C. Tulotta, E. Zoni, M. Kruithof-de Julio, G. Van Der Horst, G. Van Der Pluijm and B. E. Snaar-Jagalska, *Methods in cell biology*, 2017, **138**, 471-496.

8. X. Chen, Y. Li, T. Yao and R. Jia, *Frontiers in Cell and Developmental Biology*, 2021, **9**, 616551.
9. D. Hill, L. Chen, E. Snaar-Jagalska and B. Chaudhry, *F1000Research*, 2018, **7**, 1682.
10. K. Szaciłowski, W. Macyk, A. Drzewiecka-Matuszek, M. Brindell and G. Stochel, *Chemical reviews*, 2005, **105**, 2647-2694.
11. Y. Chen, L. Bai, P. Zhang, H. Zhao and Q. Zhou, *Molecules*, 2021, **26**, 5679.
12. J. F. Machado, J. D. G. Correia and T. S. Morais, *Molecules*, 2021, **26**, 3153.
13. A. Juzeniene, K. P. Nielsen and J. Moan, *Journal of environmental pathology, toxicology and oncology*, 2006, **25**.
14. A. Li, R. Yadav, J. K. White, M. K. Herroon, B. P. Callahan, I. Podgorski, C. Turro, E. E. Scott and J. J. Kodanko, *Chemical Communications*, 2017, **53**, 3673-3676.
15. J. D. Knoll, B. A. Albani, C. B. Durr and C. Turro, *The Journal of Physical Chemistry A*, 2014, **118**, 10603-10610.
16. J. D. Knoll, B. A. Albani and C. Turro, *Accounts of chemical research*, 2015, **48**, 2280-2287.
17. E. Wachter, D. K. Heidary, B. S. Howerton, S. Parkin and E. C. Glazer, *Chemical communications*, 2012, **48**, 9649-9651.
18. H. D. Cole, J. A. Roque III, G. Shi, L. M. Lifshits, E. Ramasamy, P. C. Barrett, R. O. Hodges, C. G. Cameron and S. A. McFarland, *Journal of the American Chemical Society*, 2021, **144**, 9543-9547.
19. Y. Chen, Y. Gao, Y. Li, K. Wang and J. Zhu, *Journal of Materials Chemistry B*, 2019, **7**, 460-468.
20. Z. Wang, R. Ma, L. Yan, X. Chen and G. Zhu, *Chemical communications*, 2015, **51**, 11587-11590.
21. W. Fan, P. Huang and X. Chen, *Chemical Society Reviews*, 2016, **45**, 6488-6519.
22. X. Li, J. F. Lovell, J. Yoon and X. Chen, *Nature Reviews Clinical Oncology*, 2020, **17**, 657-674.
23. R. S. Narayan, P. Molenaar, J. Teng, F. M. Cornelissen, I. Roelofs, R. Menezes, R. Dik, T. Lagerweij, Y. Broersma and N. Petersen, *Nature communications*, 2020, **11**, 1-14.
24. R. J. Tallarida, *Genes & cancer*, 2011, **2**, 1003-1008.
25. M. N. Fukuda, C. Ohyama, K. Lowitz, O. Matsuo, R. Pasqualini, E. Ruoslahti and M. Fukuda, *Cancer research*, 2000, **60**, 450-456.
26. J. Zhang, H. Spring and M. Schwab, *Cancer letters*, 2001, **171**, 153-164.
27. V. I. Romanov, D. B. Durand and V. A. Petrenko, *The Prostate*, 2001, **47**, 239-251.
28. L. M. Haugaard-Kedstrom, L. S. Clemmensen, V. Sereikaite, Z. Jin, E. F. Fernandes, B. Wind, F. Abalde-Gil, J. Daberger, M. Vistrup-Parry and D. Aguilar-Morante, *Journal of Medicinal Chemistry*, 2021, **64**, 1423-1434.
29. R. Binetruy-Tournaire, C. Demangel, B. Malavaud, R. Vassy, S. Rouyre, M. Kraemer, J. Plouet, C. Derbin, G. Perret and J. C. Mazie, *The EMBO journal*, 2000, **19**, 1525-1533.
30. D.-G. Bae, Y.-S. Gho, W.-H. Yoon and C.-B. Chae, *Journal of Biological Chemistry*, 2000, **275**, 13588-13596.
31. T. Asai, M. Nagatsuka, K. Kuromi, S. Yamakawa, K. Kurohane, K. Ogino, M. Tanaka, T. Taki and N. Oku, *FEBS letters*, 2002, **510**, 206-210.
32. C. Díaz-Perlas, M. Varese, S. Guardiola, M. Sánchez-Navarro, J. García, M. Teixidó and E. Giralt, *ChemBioChem*, 2019, **20**, 2079-2084.
33. Z. Han, Z. Zhou, X. Shi, J. Wang, X. Wu, D. Sun, Y. Chen, H. Zhu, C. Magi-Galluzzi and Z.-R. Lu, *Bioconjugate chemistry*, 2015, **26**, 830-838.
34. L. T. Brinton, D. K. Bauknight, S. S. K. Dasa and K. A. Kelly, *PLoS One*, 2016, **11**, e0155244.
35. N. U. Dharmaratne, A. R. Kaplan and P. M. Glazer, *Cells*, 2021, **10**, 541.
36. Z. Wu, S. Newstead and P. C. Biggin, *Scientific Reports*, 2020, **10**, 1-12.
37. D. Rotin, B. Robinson and I. F. Tannock, *Cancer research*, 1986, **46**, 2821-2826.
38. M. Soltani, M. Souri and F. Moradi Kashkooli, *Scientific Reports*, 2021, **11**, 19350.
39. M. Kanamala, W. R. Wilson, M. Yang, B. D. Palmer and Z. Wu, *Biomaterials*, 2016, **85**, 152-167.